Investigation of properties of surface modes at the boundary of DNA origami lattice

Thanos Ioannidis[1], Tatjana Gric[1,2,3], Edik Rafailov[2,4]

[1] *Department of Electronic Systems, Vilnius Gediminas Technical University, Vilnius, Lithuania*
[2] *Aston Institute of Photonic Technologies, Aston University, Birmingham B4 7ET, UK*
[3] *Semiconductor Physics Institute, Center for Physical Sciences and Technology, Vilnius, Lithuania*
[4] *Peter the Great St. Petersburg Polytechnic University, St. Petersburg, Russia*
*[*tatjana.gric@vgtu.lt](mailto:tatjana.gric@vgtu.lt)*

Herein, the models for the DNA origami lattice will be investigated. Our aim is to theoretically explore the ways of constructing DNA origami. To achieve this goal the DNA origami structure consisting of nanowires embedded in a host material will be treated from the perspective of nanowire metamaterial. Surface plasmon polaritons propagating at the interface of air and DNA metamaterial are analyzed and the ways of assembling DNA origami are theoretically investigated. The dispersion relation is attained by means of the transfer matrix technique and employing continuity conditions of electric fields and its derivatives at the boundary separating two regions. We have concluded that with the involvement of the larger amount of the nanowires into the metamaterial unit cell frequencies of surface plasmon polaritons are altered towards higher frequency range. Doing so, in this work, we have studied the effect of modifications of the metamaterial allowing for the shift of the dispersion maps towards higher frequencies. In this relation, it is possible to obtain propagation of spoof plasmons mimicking the behavior of surface waves at lower frequencies.

1. Introduction

DNA origami technology has been increasingly expanding its application fields such as nano-engineering, medical science and drug delivery, nano-chemistry, and robotics. Among them bio-mimetics and molecular robotics are cutting edge topics for researchers these days.

Latest advances in the field of nanotechnology have provided a fertile ground for a diverse toolbox of nanoobjects possessing arbitrary shapes, sizes and material properties. Nanoparticles and nanostructured metamaterials have attracted interest in the scientific community because of their tunable physiochemical characteristics such as melting point, wettability, electrical and thermal conductivity, catalytic activity, light absorption and scattering resulting in enhanced performance over their bulk counterparts. Though, there is still need for the effective strategies aiming to engineer and tune their properties [1, 2]. It is worthwhile mentioning, that it is challenging and costly process to manufacture predefined, highly ordered structures by means of conventional top-down nanofabrication procedures. Colloidal lithography is an example of the technique to pattern large-scale two dimensional ordered nanostructure arrays [3-5]. A typical bottom-up method such as self-assembly of block copolymer has gained prominence in fabrication of highly ordered nanostructures in recent years, since it can access extremely dense and complex nanostructures over a large area for device applications [6, 7]. However, bottom-up approaches relying on self-assembly have arisen as attractive low-cost options [8, 9]. Different biomolecules, such as DNA [10, 11], proteins [12, 13], peptides [14, 15] and lipids [16], have been employed as self-assembling components. DNA stands for as the most promising option aiming to achieve the predetermined goals because of its exceptional chemical and biological properties [17, 18].

Molecular self-assembly based on DNA stands for as a convincing attitude aiming to design structurally flexible, well-defined and highly addressable nano- and microscale objects [18-20]. Especially, custom-designed DNA-based motifs can nowadays be easily manufactured and applied in different appliances such as drug delivery [22, 23], plasmonics [24-26] because of the creation of the DNA origami method [21]. Furthermore, DNA nanostructures have been utilised to direct higher-ordered arrangements of DNA-functionalized metal nanoparticles [27, 28]. Geometrically ordered

structures of Au nanoparticles and other metal nanoparticles possess exceptional physical properties, and therefore provide a fertile ground for a variety of applications [29, 30].

DNA origami stands for as one of the most effective approaches to construct DNA compounds. In this relation, a long single-stranded DNA scaffold is folded into a predefined structure via the cooperative action of dozens of complimentary single-stranded oligonucleotides. The DNA origami techniques open the wide avenues for the construction of practically any arbitrary two- or three dimensional nanostructure [31, 32]. Moreover, the DNA origami compounds carry a high overall negative (surface) charge because of the sugar-phospate backbone of the DNA molecule. The former makes them appropriate elements in electrostatic self-assembly. Aiming to electrostatically assemble lamellar nanowires, DNA origami compounds have been utilized in conjunction with positively charged collagen-mimetic peptides [33]. DNA origami compounds can be complexed with cationic structures in a feasible way based on the previous studies, in which DNA origami have been electrostatically coated with virus capsid proteins [34], cationic polymers [35-38], chitosan and protein-dendron conjugated.

One can mold DNA into nearly any 2D and 3D shapes via molecular folding (i.e. DNA origami). Moreover, it was concluded that DNA origami can be crystallized into 3D superlattices over large areas. Doing so, superlattices could be formed by 3D crystallization of DNA origami. It is worthwhile noting, that the former have not been constructed thus far. Metamaterials are artificial substances that are structurally engineered to have properties not typically found in nature. To date, almost all metamaterials have been made from inorganic materials such as silicon and copper, which have unusual electromagnetic or acoustic properties that allow them to be used, for example, as invisible cloaks, superlenses or super absorbers for sound. Here, we show that metamaterials with unusual properties can be prepared using DNA as a building block. The models for the DNA origami lattice will be investigated in this work. It is worthwhile mentioning, that the set of the DNA origami lattices has been considered in the frame of the present work. Doing so, the tunability features were considered by modifying the DNA origami lattice. The dramatic impact of the chosen DNA origami model on the propagation of surface plasmon polaritons has been investigated. The main goal of this study is to theoretically explore the possibility of constructing DNA origami. In this relation we will investigate the DNA origami model consisting of metal nanowires embedded in a host dielectric media. The structure under consideration will be treated form the perspectives of the nanowire metamaterials theory.

2. Theoretical formulation

Boundary separating the DNA origami lattice [39] and dielectric is shown in Fig. 1. It should be mentioned, that every inclusion only interacts with another as a macroscopic source. The DNA origami lattice is constructed artificially by employing the inclusions embedded in a dielectric. Inclusions described by the permittivity ε_m are embedded in a dielectric with permittivity ε_d. It should be noted, that unit cell of the origami lattice possesses a hexagonal shape. The presented design is feasible by utilizing DNA origami nanostructures that can be used to guide the higher-order arrangement of the nanowires in a monitored and programmable manner. In this relation, the compound under consideration stands for as a promising tool for further applications.
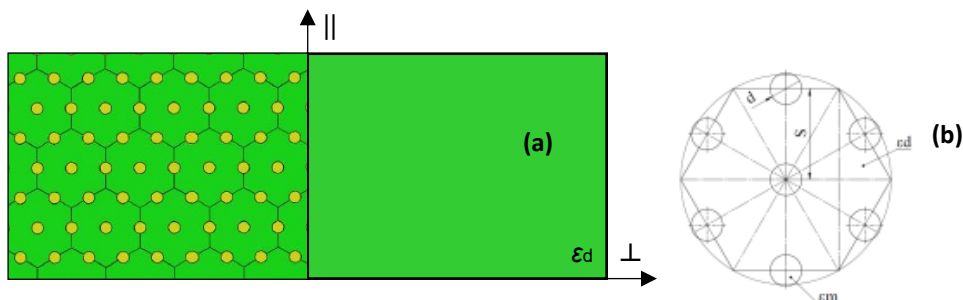
Fig. 1. A schematic view of the boundary separating DNA origami lattice and a dielectric medium (a); a hexagonal unit cell (b)

The dielectric properties of the DNA origami lattice in different directions are described by means of the Maxwell-Garnett effective medium approximation [40] and are derived starting from Schrodinger's Wave Equation:

$$\varepsilon_\perp = \varepsilon_d \left[\frac{\varepsilon_m (1+\rho) + \varepsilon_d (1-\rho)}{\varepsilon_m (1-\rho) + \varepsilon_d (1+\rho)} \right]$$

(1)

$$\varepsilon_\parallel = \varepsilon_m \rho + \varepsilon_d (1-\rho)$$

(2)

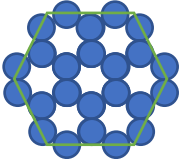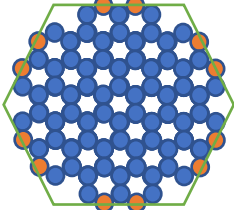Here, ρ is the metal filling fraction factor calculated as follows:
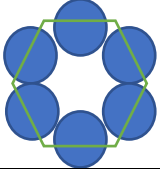
$$\rho = \frac{nanowire\ area}{unit\ cell\ area}$$

(3)

A Drude model is adopted aiming to investigate the particularities of the surface waves and to describe the metal (i. e. silver). Doing so, permittivity is expressed as $\varepsilon_m(\omega) = \varepsilon_\infty - \frac{\omega_p^2}{\omega^2 + i\delta\omega}$. The properties are found by matching this permittivity function to a particular frequency range of bulk material [41]. It is concluded [42] that for silver, the values of $\varepsilon_\infty = 5$, $\omega_p = 9.5eV = 2.30 \cdot 10^{15}\ Hz$, $\delta = 0.0987eV = 2.39 \cdot 10^{13}\ Hz$ give a reasonable fit. By making an assumption that DNA origami lattice unit cell has a hexagonal form, we determine the metal filling fraction (ρ). These calculations are dramatically influenced by the estimates of the wires diameter (d) and spacing (S) as follows [43]:

$$\rho = \frac{\pi d^2}{2\sqrt{3}S^2}$$

(4)

The expressions of the filling fractions for the novel metamaterial unit cells are presented in Table 1. We can define the fill fraction of nanowires (ρ) in the host material by Eq. (3).

Table 1. Expressions of the filling ratio, ρ for different geometry of the metamaterial unit cell.

Geometry of the metamaterial unit cell	Filling ratio, ρ	Case
	$\rho = \frac{3\pi d^2}{8\sqrt{3}S^2}$	S3
	$\rho = \frac{9\pi d^2}{4\sqrt{3}S^2}$	S18
	$\rho = \frac{39\pi d^2}{4\sqrt{3}S^2}$	S78

3. Results and discussions

With the use of Eqs. 1, 2, effective permittivities of the metamaterial are computed for the cases composed by employing different types of the cells as listed in Table 1. The parameters used in the calculations are $\varepsilon_d = 11.8$, $d = 40nm$, $S = 70nm$. Fig. 2 shows dependencies of the permittivity components upon frequency for different geometry of the metamaterial unit cell.
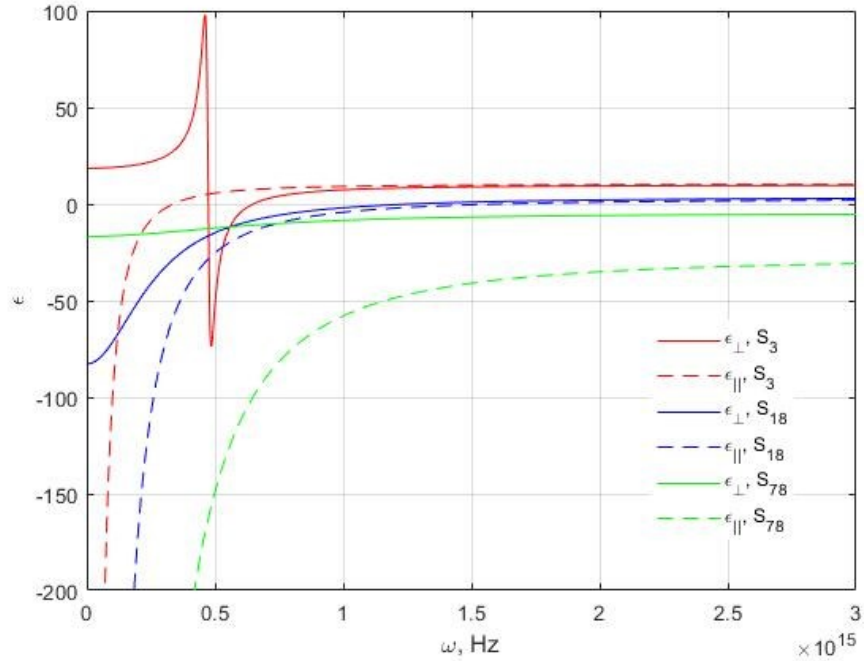

Fig. 2. Influence of the DNA lattice geometry upon the effective dielectric parameters.

In Fig. 2, the effective medium constants for the DNA compound are plotted. The DNA lattice exhibits an epsilon-near-zero effect as well as epsilon-near-pole resonance for S3 case only. Only the real parts are presented for clarity and the imaginary parts can be calculated similarly. Type I behavior, which is difficult to achieve with multilayer structures, is demonstrated for S3 case. It is worthwhile noting, that material behaves as an effective metal ($\varepsilon_{\parallel}, \varepsilon_{\perp} < 0$) in case of S18, S78 instances. Despite the fact, that medium in S18 case behaves as a conventional metal, dispersion maps of surface waves possess some peculiarities, i.e. higher order modes exist at the frequency range under consideration.

Fig. 3 demonstrates the dispersion curves of surface plasmon polaritons (SPPs) for different geometry of the metamaterial unit cell. On the x-axis, β is depicted and on y-axis, frequency is plotted. It is found that surface modes are obtained in structure under investigation for S3 and S18 cases.

It is evident that if number of the nanowires employed in the metamaterial unit cell increases the frequency of surface modes shifts toward higher frequency range.
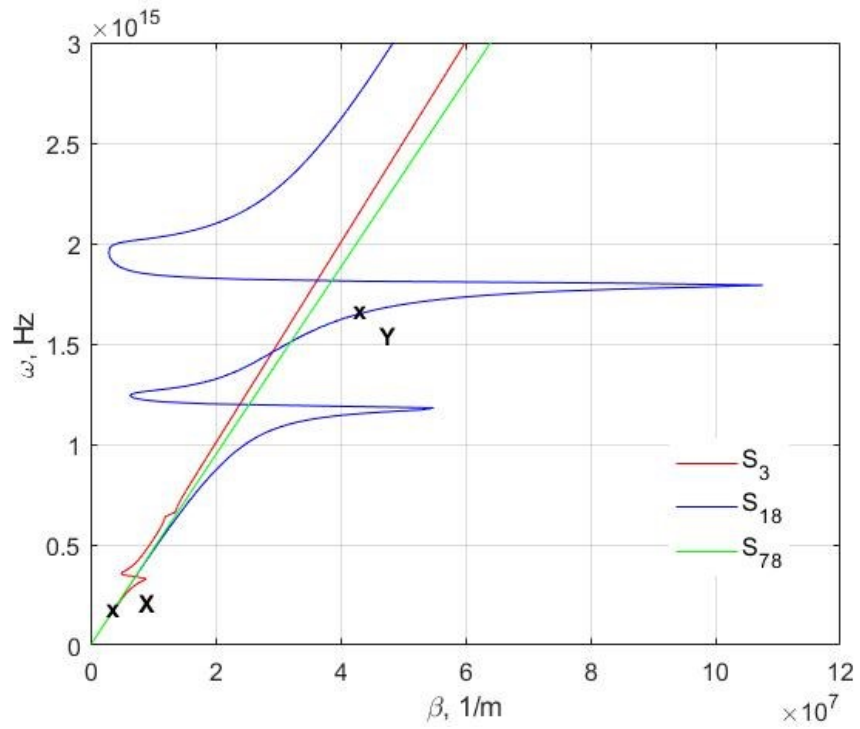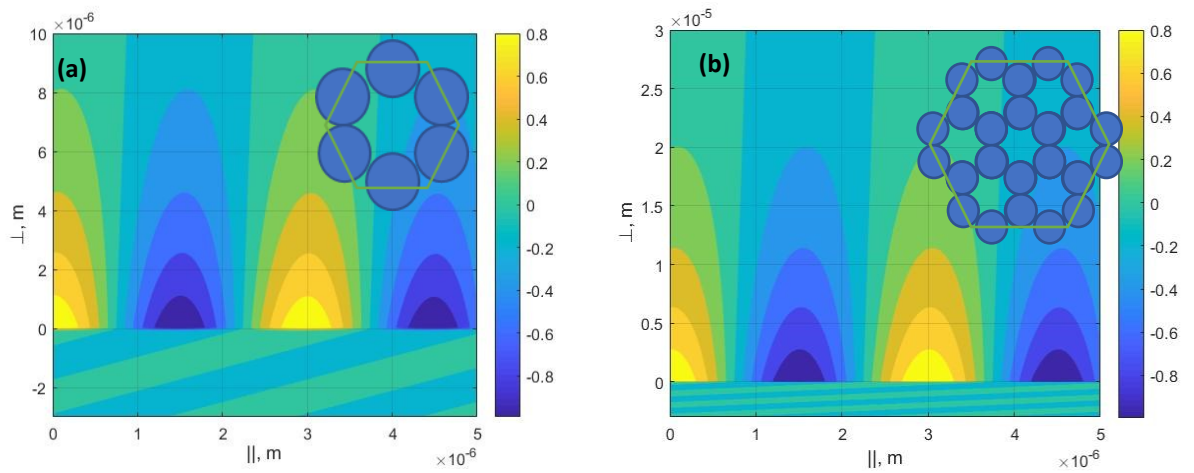
Fig. 3. Dispersion maps of surface modes at the interface of metamaterial and dielectric.

To demystify the nature of surface modes, electric field profiles of surface modes corresponding to points 'x' and 'y' are shown in Fig. 4. The field intensity distribution shown in Figure 4 exhibits high field enhancement near the interface.
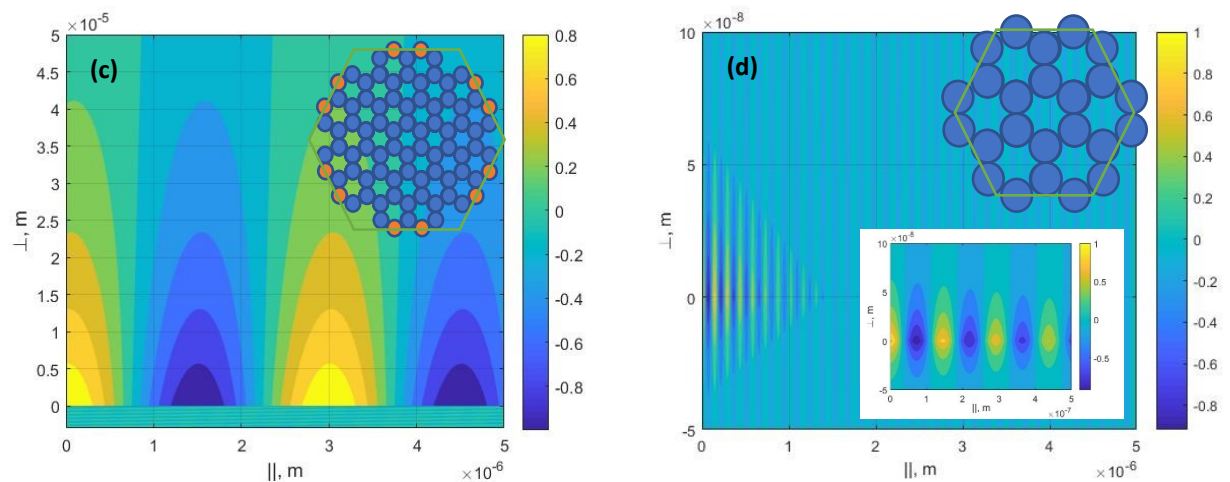
Fig. 4. Electric field profiles: (a) $f = 0.1 \cdot 10^{15} \, Hz$, S3 (point 'X' in Fig. 3), (b) $f = 0.1 \cdot 10^{15} \, Hz$, S18 (point 'X' in Fig. 3), (c) $f = 0.1 \cdot 10^{15} \, Hz$, S78 (point 'X' in Fig. 3), (d) $f = 1.65 \cdot 10^{15} \, Hz$, S18 (point 'Y' in Fig. 3). Here, || and ⊥ correspond to the axis of structure (Fig. 1). The enlarged view is shown in the inset of Fig. 4d.

Conclusions

The designs for the DNA origami lattice have been presented in this work. In the present paper, effect of the metamaterial unit cell on the dispersion properties, electric field distributions of SPPs propagating at the interface of air, and the metamaterial are studied. It is found that geometry of the metamaterial unit cell is an important factor dramatically affecting properties of surface waves. It is found that with increase in the number of nanowires composing the metamaterial unit cell surface modes frequency increases. Hence, by selecting suitable values of these parameters, frequency range of SPPs can be improvised in the required frequency range. Doing so, we end up with a typical example is "spoof" SPPs, which mimic features of SPPs without penetrating into the structure, but only with periodic corrugations on the surfaces. They hold considerable promise in device applications from microwaves to the far infrared, where real SPP modes do not exist.

Acknowledgement

References:

1. K. J. M. Bishop, C. E. Wilmer, S. Soh and B. A. Grzybowski, Small, 2009, 5, 1600–1630.
2. Z. Nie, A. Petukhova and E. Kumacheva, Nat. Nanotechnol., 2010, 5, 15–25.
3. G. Zhang and D. Wang, Chem. Asian J., 2009, 4(2), 236–245.
4. Y. Li, W. Cai, and G. Duan, Chem. Mater., 2008, 20(3), 615–624.
5. N. Vogel, C. K. Weiss, and K. Landfester, Soft Matter., 2012, 8(15), 4044.
6. N. Vourdas, D. Kontziampasis, G. Kokkoris, et. al., Nanotechnology, 2010, 21, 085302.
7. S. M. Park, X. Liang, B. D. Harteneck, et. al., ACS Nano, 2011, 5, 8523–8531.
8. H. Li, J. D. Carter and T. H. LaBean, Mater. Today, 2009, 12, 24–32.
9. A. Biswas, I. S. Bayer, A. S. Biris, T. Wang, E. Dervishi and F. Faupel, Adv. Colloid Interface Sci., 2012, 170, 2–27.

10. N. C. Seeman, Nature, 2003, 421, 427–431.
11. M. R. Jones, N. C. Seeman and C. A. Mirkin, Science, 2015, 347, 1260901.
12. M. Uchida, M. T. Klem, M. Allen, P. Suci, M. Flenniken, E. Gillitzer, Z. Varpness, L. O. Liepold, M. Young and T. Douglas, Adv. Mater., 2007, 19, 1025–1042.
13. Q. Luo, C. Hou, Y. Bai, R. Wang and J. Liu, Chem. Rev., 2016, 116, 13571–13632.
14. J. Wang, K. Liu, R. Xing and X. Yan, Chem. Soc. Rev., 2016, 45, 5589–5604.
15. D. M. Raymond and B. L. Nilsson, Chem. Soc. Rev., 2018, 47, 3659–3720.
16. M. Antonietti and S. Förster, Adv. Mater., 2003, 15, 1323–1333.
17. F. A. Aldaye, A. L. Palmer and H. F. Sleiman, Science, 2008, 321, 1795–1799.
18. F. Hong, F. Zhang, Y. Liu and H. Yan, Chem. Rev., 2017, 117, 12584–12640.
19. N. C. Seeman and H. F. Sleiman, Nat. Rev. Mater., 2017, 3, 17068.
20. S. Nummelin, J. Kommeri, M. A. Kostiainen and V. Linko, Adv. Mater., 2018, 30, 1703721.
21. P. W. K. Rothemund, Nature, 2006, 440, 297–302.
22. J. Li, C. Fan, H. Pei, J. Shi and Q. Huang, Adv. Mater., 2013, 25, 4386–4396.
23. V. Linko, A. Ora and M. A. Kostiainen, Trends Biotechnol., 2015, 33, 586–594.
24. A. Kuzyk, R. Schreiber, Z. Fan, G. Pardatscher, E. M. Roller, A. Högele, F. C. Simmel, A. O. Govorov and T. Liedl, Nature, 2012, 483, 311–314.
25. B. Shen, V. Linko, K. Tapio, S. Pikker, T. Lemma, A. Gopinath, K. V. Gothelf, M. A. Kostiainen and J. J. Toppari, Sci. Adv., 2018, 4, eaap8978.
26. N. Liu and T. Liedl, Chem. Rev., 2018, 118, 3032–3053.
27. N. C. Seeman and O. Gang, MRS Bull., 2017, 42, 904–912.
28. S. Julin, S. Nummelin, M. A. Kostiainen and V. Linko, J. Nanopart. Res., 2018, 20, 119.
29. K. V. Gothelf, MRS Bull., 2017, 42, 897–903.
30. Y. Ofir, B. Samanta and V. M. Rotello, Chem. Soc. Rev., 2008, 37, 1814–1825.
31. S. M. Douglas, H. Dietz, T. Liedl, B. Högberg, F. Graf and W. M. Shih, Nature, 2009, 459, 414–418.
32. C. E. Castro, F. Kilchherr, D. N. Kim, E. L. Shiao, T. Wauer, P. Wortmann, M. Bathe and H. Dietz, Nat. Methods, 2011, 8, 221–229.
33. T. Jiang, T. A. Meyer, C. Modlin, X. Zuo, V. P. Conticello and Y. Ke, J. Am. Chem. Soc., 2017, 139, 14025–14028.
34. J. Mikkilä, A. P. Eskelinen, E. H. Niemelä, V. Linko, M. J. Frilander, P. Törmä and M. A. Kostiainen, Nano Lett., 2014, 14, 2196–2200.
35. J. K. Kiviaho, V. Linko, A. Ora, T. Tiainen, E. Järvihaavisto, J. Mikkilä, H. Tenhu, Nonappa and M. A. Kostiainen, Nanoscale, 2016, 8, 11674–11680.
36. N. P. Agarwal, M. Matthies, F. N. Gür, K. Osada and T. L. Schmidt, Angew. Chem., Int. Ed., 2017, 56, 5460–5464.
37. N. Ponnuswamy, M. M. C. Bastings, B. Nathwani, J. H. Ryu, L. Y. T. Chou, M. Vinther, W. A. Li, F. M. Anastassacos, D. J. Mooney and W. M. Shih, Nat. Commun., 2017, 8, 15654.
38. Y. Ahmadi, E. De Llano and I. Barišić, Nanoscale, 2018, 10, 7494–7504.
39. T. Gric, Pr. Electromagn. Res., 2016, M 46, 165–172.
40. P. Shekhar, J. Atkinson and Z. Jacob, Nano Convergence, 2014, 1, 14.
41. P. B. Johnson, R. W. Christy, 1972, Phys. Rev. B 6, 4370.
42. C. Oubre, P. Nordlander, J. Phys. Chem. B, 2005, 109(20), 10042-10051.
43. R. Starko-Bowes, J. Atkinson, W. Newman, H. Hu, T. Kallos, G. Palikaras, R. Fedosejevs, S. Pramanik, Z. Jacob, J. Opt. Soc. Am. B, 2015, 32(10), 2074-2080.